List of Tables

Blank Page

2.1.3.3.1 In-Containment Refueling Water Storage Tank

The function of the IRWST is to maintain a large reserve of borated water at a homogeneous concentration and temperature. The borated water is used to flood the refueling cavity for normal refueling. It is also the safety-related source of water for emergency core cooling in the event of a LOCA and is a source of water for containment cooling and for core melt cooling in the event of a severe accident. The IRWST represents the lowest point in the containment and communicates with the remainder of the containment such that any water discharged from the RCS will drain back into the IRWST.

Each of the four SIS (safety-related) and one SAHRS (non-safety-related) train is provided with a separate sump suction connection to the IRWST. To prevent RCS thermal insulation and other debris from reducing the suction head of the SIS and SAHRS pumps, a series of barriers is used to minimize the amount of debris which can reach the sumps, including a back-flushing function provided by the SAHRS.

2.1.3.3.2 Safety Injection

Safety injection within the U.S. EPR is performed by an MHSI system, an LHSI system, and four accumulators. These safety-related systems consist of 4x100% independent trains that are physically separated and protected within the safeguard buildings. The MHSI system draws borated water from the IRWST and injects it into the cold leg at a pressure lower then the main steam safety valve (MSSV) setpoints to ensure that in the event of a steam generator tube rupture (SGTR), primary inventory cannot be released directly to the environment. The four accumulators are connected to the RCS cold legs and provide injection when the RCS pressure falls below the corresponding setpoint.

2.1.3.3.3 Residual Heat Removal

The RHR system is combined with the LHSI system; however, different operating configuration is used to transfer residual heat to the plant cooling water systems. The RHR system of each plant safety train includes suction on the hot leg of each RCS loop

considered within the system. Given the long lead time expected prior to any SAHRS actuation, this system is consider sufficiently reliable with a single train.

The SAHRS has four primary modes of operation, each playing a role in controlling the environmental conditions within the containment so that its fission product retention function is maintained. These modes of SAHRS operation include:

- Passive cooling of molten core debris
- Active spray for environmental control of the containment atmosphere
- Active recirculation cooling of the molten core debris and containment atmosphere
- Active back-flush of the IRWST.

The SAHRS train is located in a dedicated, radiologically-controlled room within one of the four plant safeguard buildings. The SAHRS train includes:

- A dedicated suction line from the IRWST
- Containment isolation valves
- A pump to support active recirculation
- A heat exchanger for containment heat rejection
- Discharge lines to a containment spray header, the spreading room, and sump screen
- Support from a dedicated cooling chain via plant auxiliary systems.

The SAHRS heat exchangers transfer the residual heat from the containment to the ultimate heat sink via dedicated portions of Component Cooling Water (CCW) and Essential Service Water (ESW) trains. During operation, the three possible flow paths downstream of the pump and the heat exchanger are:

1. To a containment spray system with a ring header and spray nozzles

2. To the spreading area of the CMSS

3. To a sump screen flushing device which is used to remove accumulated debris.

The general configuration of the SAHRS train is provided in Figure 2-23.

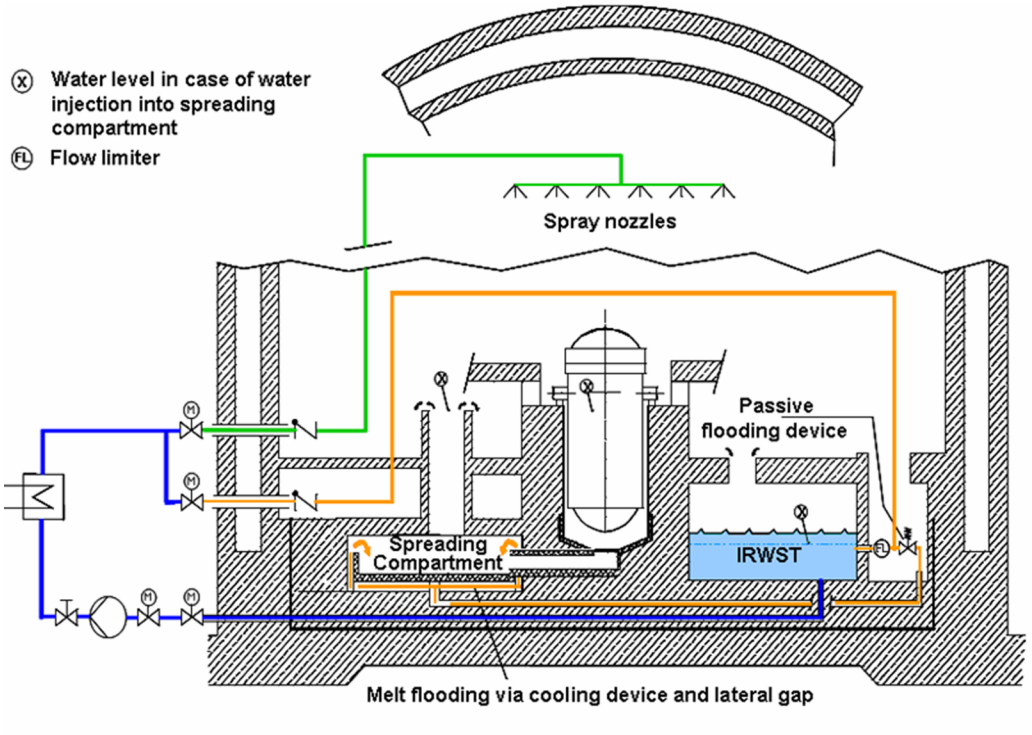

Figure 2-23 Severe Accident Heat Removal System

2.2.4.1 *Passive Cooling of Core Debris*

As discussed in Section 2.2.3, the U.S. EPR includes a CMSS to stabilize molten core debris resulting from a severe accident. The SAHRS provides the cooling water to the cooling structure used for melt stabilization as described in Section 2.2.3.4. Once molten core debris is within the spreading compartment, water from the IRWST will passively start to fill the cooling structure. This dedicated flooding line is equipped with a flow limiter downstream of the IRWST outlet, which limits the flow to around 13,000 lb/min. This expected flow rate fills the cooling structure within five minutes. Water then

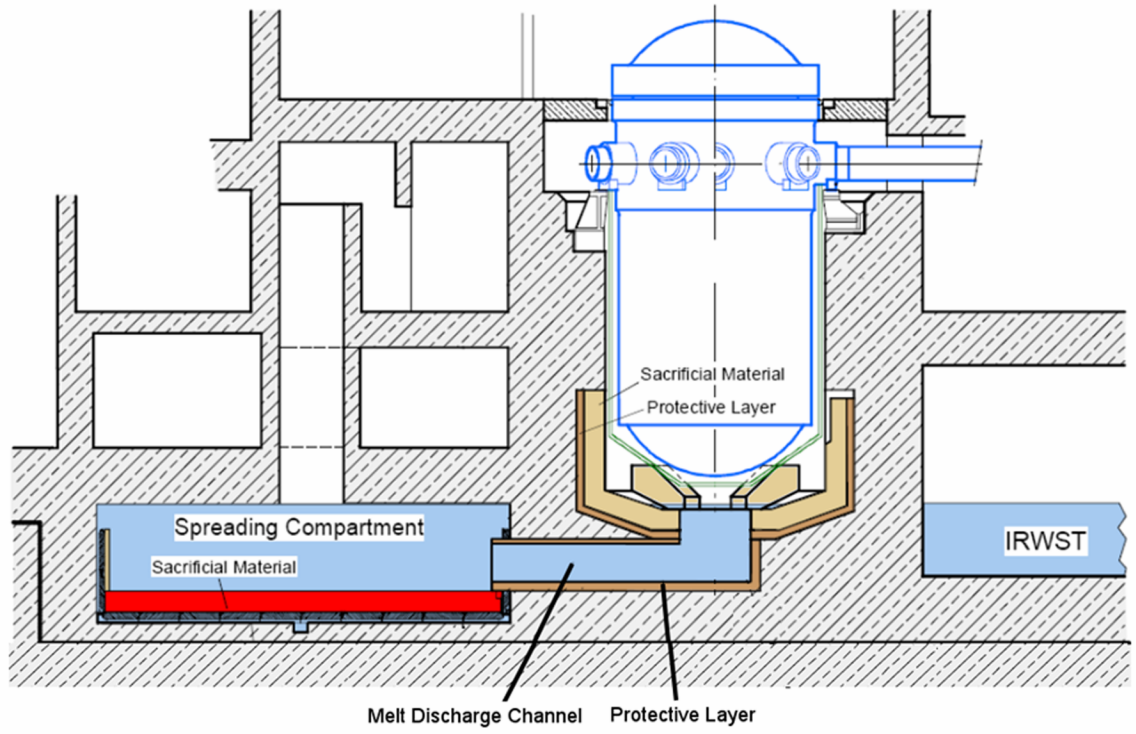

Figure 2-25 Active Melt Retention System Cooling

2.2.4.4 *IRWST Backflush*

The final mode of operation of the SAHRS is to provide a back-flushing function within the IRWST. Operation in this mode serves to dislodge any debris from the sump strainers that might compromise the ability of the SAHRS to draw water from the IRWST. Only a fraction of the SAHRS is used for back-flushing; therefore, the system can operate in this mode while continuing operation in another containment cooling mode.

2.2.4.5 *SAHRS Dedicated Cooling Chain*

To support the active heat removal modes of the SAHRS, dedicated portions of the CCW and ESW systems are used to form a dedicated cooling chain to transfer heat to the ultimate heat sink. These dedicated cooling trains are composed of a non-safety CCW and ESW train for the one SAHRS train. This cooling chain is dedicated to severe accident operation and is not used to support normal plant operations or mitigate the

- *Actuation of Hydrogen Mixing Dampers*. Provides the ability to open the mixing dampers either automatically on measured containment pressure or manually from the control room.

- *Position Indication of Hydrogen Mixing Dampers*. Provides the ability to monitor the state of the mixing dampers.

2.2.5.4 *Monitoring of Containment Heat Removal*

As discussed in Section 2.2.4, the U.S. EPR uses a SAHRS to control the long-term, post-accident, environmental conditions within the containment. To control containment pressure, the system is operated in an active mode with either a containment spray or long-term recirculation. This system is manually started on a defined containment pressure and supported by the dedicated cooling chain as described in 2.2.4.5. The U.S. EPR includes the following provisions to monitor containment heat removal:

- *Measurement of Containment Pressure*. Provided to identify the need for active containment cooling.

- *Measurement of IRWST Temperature*. Provided to monitor system performance during operation.

- *Measurement of SAHRS Heat Exchanger Inlet Temperature*. Provided to monitor system performance during operation.

- *Measurement of SAHRS Heat Exchanger Outlet Temperature*. Provided to monitor system performance during operation.

- *Measurement of SAHRS Flow Rate*. Provided to monitor system performance during operation.

- *Measurement of SAHRS Sump Level*. Provided to identify fluid leakage from the SAHRS train.

phenomena through the demonstration of the U.S. EPR's severe accident response capability to the relevant severe accident events.

The remainder of this report presents the elements of this severe accident evaluation methodology for issue resolution. Specifically,

- Identification of Safety Goals, Section 4.1
- Identification of Processes and Phenomena, Section 4.2
  - A Hypothetical Phenomenologically-Bounding Severe Accident, Section 4.2.1
  - Presentation of Severe Accident Processes and Phenomena, Section 4.2.2
  - Scaling Analysis for Phenomenological Importance, Section 4.2.3
- Assessment of applicable research and development programs, Section 5.0
- Analysis Methods, Section 6.0
  - Overview of the U.S. EPR Analytical Methodology, Section 6.1
  - Code Applicability, Section 6.2
  - Validation of Analytical Tools, Section 6.3
  - Description of U.S. EPR Analytical Models, Section 6.4
  - Calculation Matrix for Safety Issue Resolution, Section 6.5
- Sample Problem Analyses, Section 7.0.

5.4.1.2 *General Overpressurization Experimentation and Discussion*

As previously described, the U.S. EPR-specific response to containment overpressurization is ultimately provided by an active spray system. This system is functionally equivalent to those present in current-generation PWRs for the mitigation of design basis LOCAs. The basis for these installed units draws on test program experience including Carolinas-Virginia Tube Reactor Containment (Reference 90) and Brookhaven National Laboratory's Containment Spray Experiments (Reference 91). The 12-hour delay allows the CGCS to perform with a high degree of reliability to fulfill its design goal of reducing hydrogen concentration to 4% in within that time.

Both the CGCS and SAHRS are highly reliable systems. The 47 independent PARs and the long lead time prior to required SAHRS actuation provide for a degree of reliability beyond that of current-generation LWRs. In traditional severe accident space, single failure is not a consideration in system design; however, the U.S. EPR severe accident systems can accommodate such a failure and still perform their function, thereby underlining the reliability of these systems.

5.4.2 *Fuel-Coolant Interactions*

FCI is a process by which molten fuel transfers its thermal energy to the surrounding coolant, leading to break-up of corium with possible formation of a coolable debris bed or potential evolution to an energetic steam explosion. Two modes of contact between the molten corium and coolant are considered:

- A pouring contact mode, where corium is poured into a pool of water. This mode could conceivably occur within the RPV when corium relocates into the water-filled lower head of the vessel.

- An injection or stratified contact mode, where a pool of corium is flooded by water. This mode can occur within the RPV as a consequence of reflood of the RPV, or later, during either molten pool formation inside the lower head or the designed flooding of the melt in the spreading area.

- SAHRS volumetric flow rate

Because the SAHRS is located in one of the safeguard buildings, the SAHRS is not exposed to any severe-accident-related conditions until its operation is initiated.

After actuation of the SAHRS, the limiting conditions (e.g., temperature, boron concentration, fission product concentration, etc.) of contaminated IRWST water flowing through the system are considered for assessing the performance of SAHRS components.

5.5.4 *Annulus*

The measurements belonging to this category are:

- Annulus pressure (subatmospheric)
- Dose rate downstream filters
- Volume flow rate downstream filters

The annulus environment is not expected to be seriously challenged during a relevant severe accident scenario as defined in Section 3.3.

MAAP4.07 is used to develop the boundary and initial conditions for defining the problems analyzed with MELTSPREAD-1.4 and WALTER. The separate-effects codes are then used to verify selected parameters used to characterize the various system performance parameters in MAAP4.07. These codes and the relationship between them in the U.S. EPR analytical methodology will be described in the following subsections.

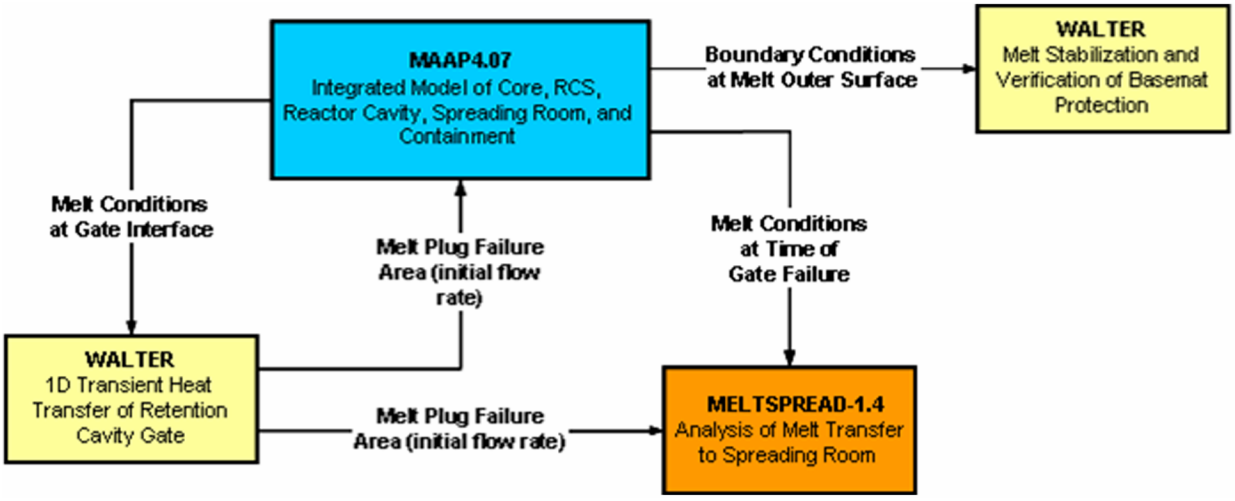

Figure 6-1 Overview of U. S. EPR Severe Accident Analytical Methodology

6.1.1 *MAAP4.07*

MAAP4 is an integral systems analysis computer code for assessing severe accidents and is developed and maintained by FAI for the EPRI. MAAP4 includes models required for analysis of a wide spectrum of severe accident phenomena that might occur within the primary system and containment. MAAP4 has the capability to simulate the progression of a severe accident sequence, including the release of fission products, from a set of initiating events to either a safe, stable state or to an impaired containment condition. MAAP4.07 is the first version of MAAP4 specifically addressing the severe accident phenomena unique to the U.S. EPR.

The basic MAAP4 code architecture consists of a main program that directs the execution through several high level subroutines. These subroutines call a sequence of

6.3 *Validation of Analytical Tools*

All three codes used for severe accident analysis in the U.S. EPR were qualified for use and application to the analysis of plant-specific severe accident phenomena. Considerable work was performed in validating the main integral code MAAP4.07 since it is used as the primary analysis tool. Most of the validation work to date has been performed by FAI, although AREVA NP has supplemented benchmarking studies related to MCCI. In addition, AREVA NP plans to continue validation work with MAAP4.07 by doing code comparison studies with other codes, such as MELCOR 1.8.6. This validation work is expected to be complete in early 2007. The validation and/or verification strategy and results for all three codes used in the U.S. EPR severe accident analytical methodology are described in this section.

6.3.1 *MAAP4.07*

The MAAP4.07 code comes with an established validation basis from its widespread use in the nuclear industry on many different plant designs. However, modifications have been made to MAAP4 in order to create version 4.07 and these modifications have been the target of additional validation studies. The main area of focus of these validation studies was in the area of MCCI since this represents the primary area of source code modifications in MAAP4.07.

FAI has performed a large number of benchmarks using MAAP4.07 to simulate various MCCI experiments. The results of these studies are summarized in this section. More important, MAAP4.07 now provides a user the ability to perform dynamic benchmarks of MCCI experiments. AREVA NP has used this new capability to perform dynamic benchmarks of two additional MCCI experiments: the CCI-2 (Reference 61) and CCI-3 (Reference 62) tests. The results of the CCI-2 and CCI-3 validation studies are also discussed in this section.

reactor cavity structures. The melt temperature predictions are important for calculation of accurate melt properties as they change with increasing MCCI, and ultimately for predicting the spreading and stabilization behavior of the melt. The agreement of the MAAP4.07 predictions of these two important parameters is sufficient validation for using MAAP4.07 in severe accident calculations involving similar types of concrete.

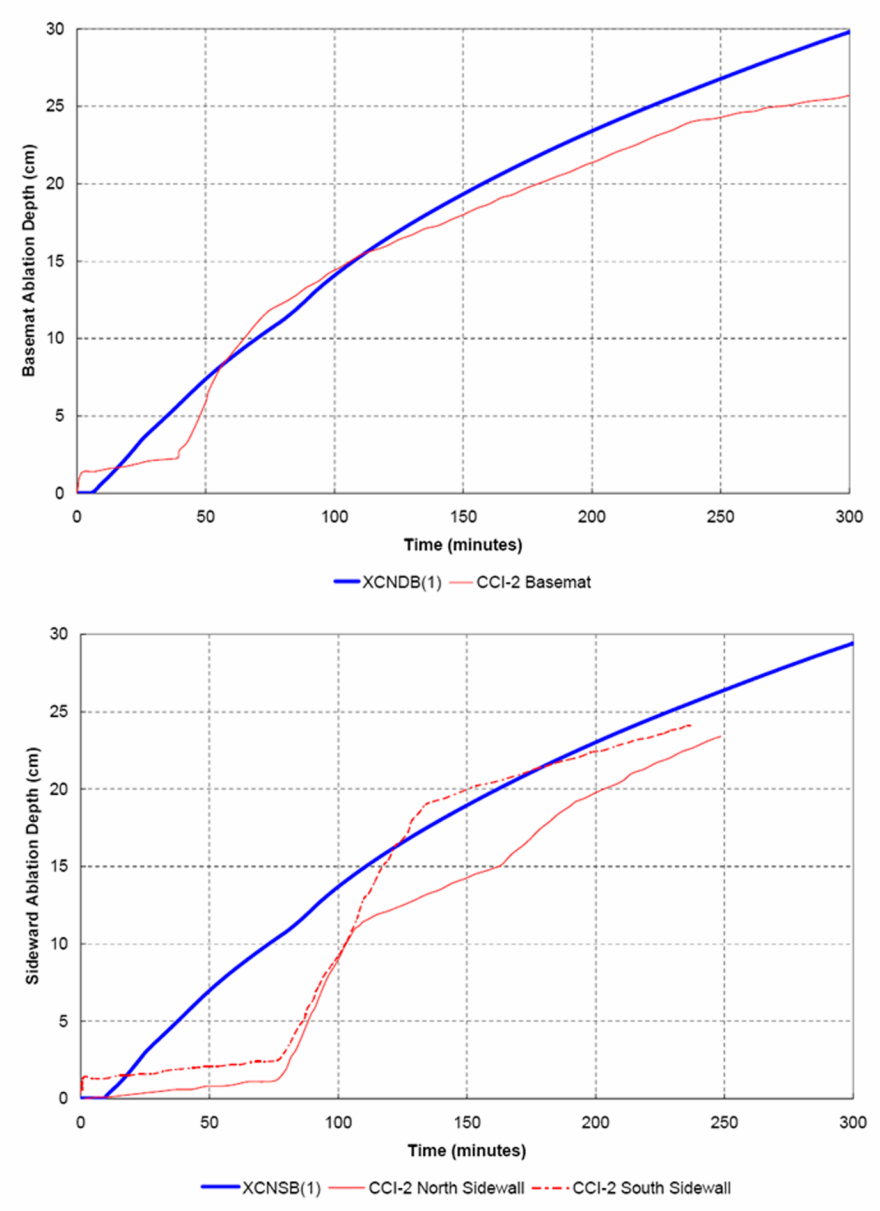

Figure 6-13 MAAP4.07 Predicted Erosion Rates vs. CCI-2 Data (top, basemat; bottom, sidewall)

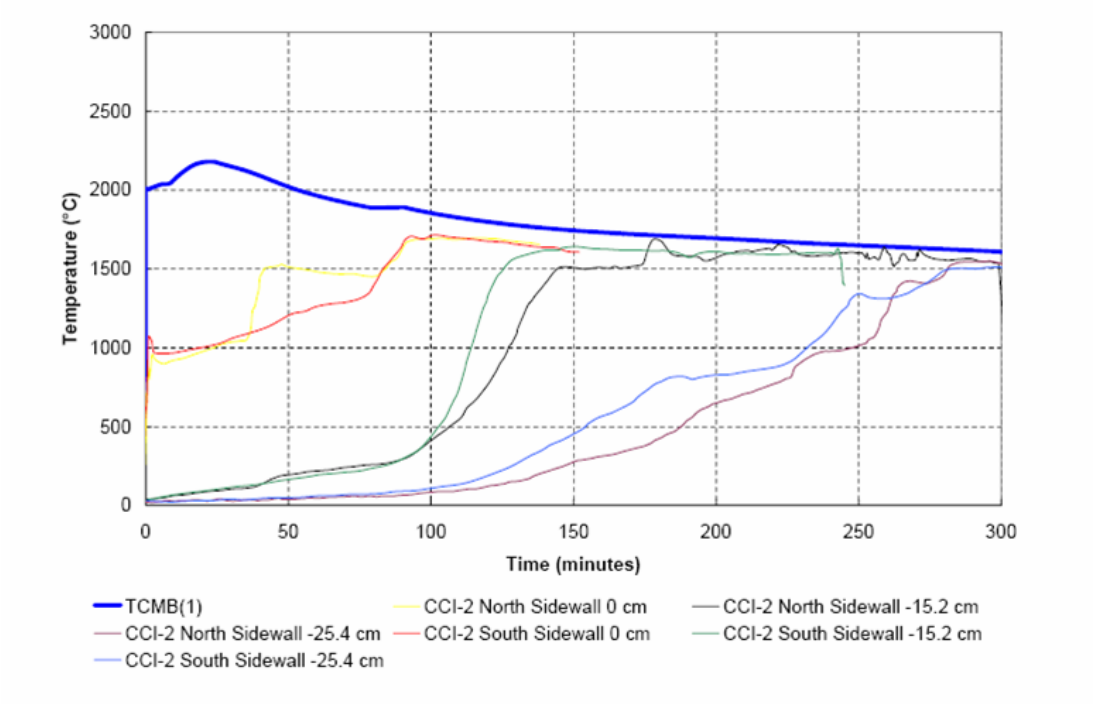

Figure 6-14 MAAP4.07 Predicted Average Melt Temperatures vs. CCI-2 Data

6.3.1.1.4 Core Concrete Interaction Experiment 3 (CCI-3)

Background

CCI-3 was a two-dimensional MCCI experiment that used much of the same test apparatus and assembly as the CCI-2 experiment. The experiment investigated MCCI for a 375-kg fully oxidized PWR core melt initially containing 15.0 wt% siliceous concrete. The details of the experimental apparatus, the test procedure, and the results are fully documented in Reference 62.

Many of the same methods that were used in the CCI-2 experiment were also employed in the CCI-3 experiment. The major differences between CCI-3 and CCI-2 were:

- Use of siliceous concrete rather than LCS concrete

- Slightly different initial debris constituent

- Slightly different initial conditions of the melt at the time of onset of ablation

Results

The CCI-3 benchmark simulation was executed for 100 minutes (6000 s). Pertinent results from the CCI-3 simulation are shown in Figure 6-15 and Figure 6-16, along with the corresponding experimental data from Reference 62. The results show fair agreement with the experimental data.

In Figure 6-15 the MAAP4.07 erosion rates for the basemat and sidewall are plotted. The CCI-3 data display some non-uniformity between the axial and radial erosion depths and the MAAP4.07 predictions lie between the two extremes. This occurs because the MAAP4.07 representation of the concrete erosion is equivalent to the average of the lateral and downward components of the real physical ablation profile.

In Figure 6-16 the MAAP4.07 average corium temperature is plotted. There is good agreement between the MAAP4.07 predicted average melt temperature and the peaks of the sidewall thermocouple responses. The basemat thermocouples register an abnormally low temperature due to the significant delay in ablation at the basemat centerline. It is unclear from the description of the CCI-3 experiment what caused the unexpected ablation delay at the basemat centerline. However, the agreement between MAAP4.07 and the melt temperatures at the sidewalls indicates accurate modeling of the melt heat transfer in the radial direction. These results demonstrate that MAAP4.07 has been validated for the calculation of MCCI involving molten pools in which the heat flux is expected to be isotropic.

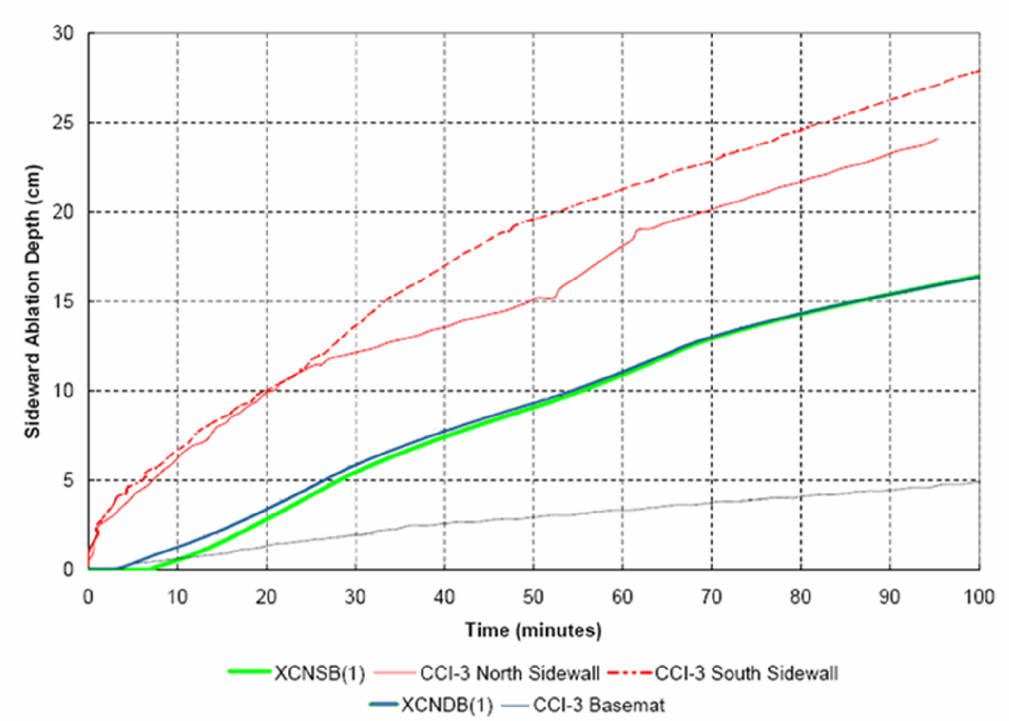

Figure 6-15 MAAP4.07 Predicted Erosion Rates vs. CCI-3 Data

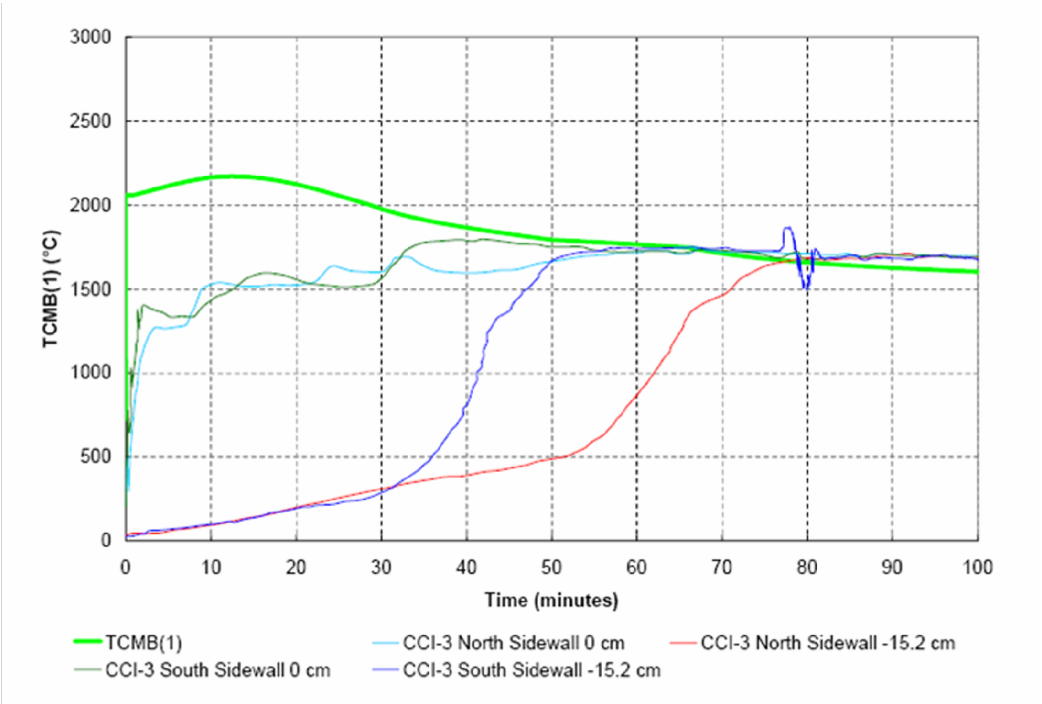

Figure 6-16 MAAP4.07 Predicted Average Melt Temperatures vs. CCI-3 Data

7.2 *Scenario Description*

The scenarios considered for the demonstration of the U.S. EPR's severe accident response are the LBLOCA, SBO (a bounding LOOP), and SBLOCA. Representative analyses were performed using both integral studies as well as more detailed, separate effect studies of certain phenomena.

7.2.1 *Integral Analysis Scenarios*

Integral analyses were performed using MAAP4 to predict the plant response to the LBLCOA, SBO, and SBLOCA scenarios. The event scenarios analyzed were run using the MAAP4 model discussed in Section 7.4 configured to run the scenarios described below.

7.2.1.1 *LBLOCA*

The initiator for the LBLOCA is a complete severance of the pressurizer surge line followed by trip of the reactor and RCPs, isolation of main feedwater (MFW), start of the emergency feedwater (EFW) and a coincident failure of all four active trains of SI. Following injection of the accumulators, the water level in the core will reach a level below the top of the active fuel. Because the active SI is unavailable, the core will start to heat up and ultimately reach the severe accident pressurization valve setpoint, signaling the start of the severe accident. The progression of this accident scenario and its associated severe accident phenomena are quantitatively described in Section 7.3.

7.2.1.2 *SBO*

The initiator for the SBO is a complete loss of all off-site sources of AC power (i.e., a LOOP), all four EDGs, and both SBO diesels. While this is an extremely remote event due to the number of AC power sources available for the U.S. EPR, it provides a bounding representation of the plant response. Given that all AC power sources are unavailable only those features that can be powered off of DC power would be available (i.e., the dedicated severe accident valves would be operable but the SI systems and active SAHRS modes would not be). Following the initiator, the reactor will trip and

MFW and EFW would not available. Following boil-off of the secondary inventory of the steam generators, the RCS temperature and pressure will start to increase until the point where the SRVs on the pressurizer will start to cycle. RCS fluid will drain into the PRT until the point that the rupture disks fail on over pressure and release inventory into the containment. The continued loss of inventory into the containment will result in core uncovery and heat up until the severe accident depressurization valve set-point is reaches signaling the start of a severe accident. The progression of this accident scenario and its associated severe accident phenomena are quantitatively described in Section 7.3.

7.2.1.3 *SBLOCA*

The initiator for the SBLOCA is a small break in the cold leg mid-loop followed by trip of the reactor and RCPs, isolation of MFW, start of EFW and a coincident failure of all four active trains of SI. Following the break, the RCS will slowly start to depressurize and empty the pressurizer. On the low pressurizer level signal, a partial cooldown via the MSRT will occur. The accumulator will inject providing inventory to cover the core and the heat from the primary system will be removed via the EFW system. Once the Condensate Storage Tanks (CST) inventory is depleted, core cooling is lost causing an increase in core temperature. Ultimately core uncovery is expected to occur resulting in a heat up until the severe accident depressurization valve setpoint is reaches signaling the start of a severe accident. The progression of this accident scenario and its associated severe accident phenomena are quantitatively described in Section 7.3.

7.2.2 *Separate Effect Analyses*

As discussed in Section 7.1, the separate effect codes MELTSPREAD and WALTER were used to model certain severe accident phenomena important to the U.S. EPR design. These phenomena were modeled using separate effect codes to allow for a more detailed analysis of the phenomena than was offered by MAAP4. These phenomena include spreading of molten core debris, failure of the reactor cavity gate, and melt stabilization of the spreading compartment cooling structure.

7.2.2.1 *Reactor Cavity Gate Failure*

Failure of the gate in the reactor cavity was modeled using the separate effects code WALTER. WALTER was used to predict the failure of the gate by determining if the 4 cm-thick aluminum gate is ablated rapidly when contacted by molten core debris. This analysis was performed in a limiting manner as opposed to modeling scenario specific timing. Therefore, the conclusions of WALTER hold for any scenario not just for the LBLOCA. Two limiting cases were run; one where the oxidic layer was resting on the aluminum plate and the other was performed with the metallic layer resting on the aluminum plate. In the case where the oxidic layer was atop the plate, the aluminum melt plug completely melts within 25 to 30 seconds after first contact with the melt (as shown in Figure 7-1 where the entire temperatures of the gate plug is above the melting temperature of aluminum). In the case where the metallic layer was atop the plate, the plug completely melts within 20 to 25 seconds after first contact with the melt (as shown in Figure 7-2).

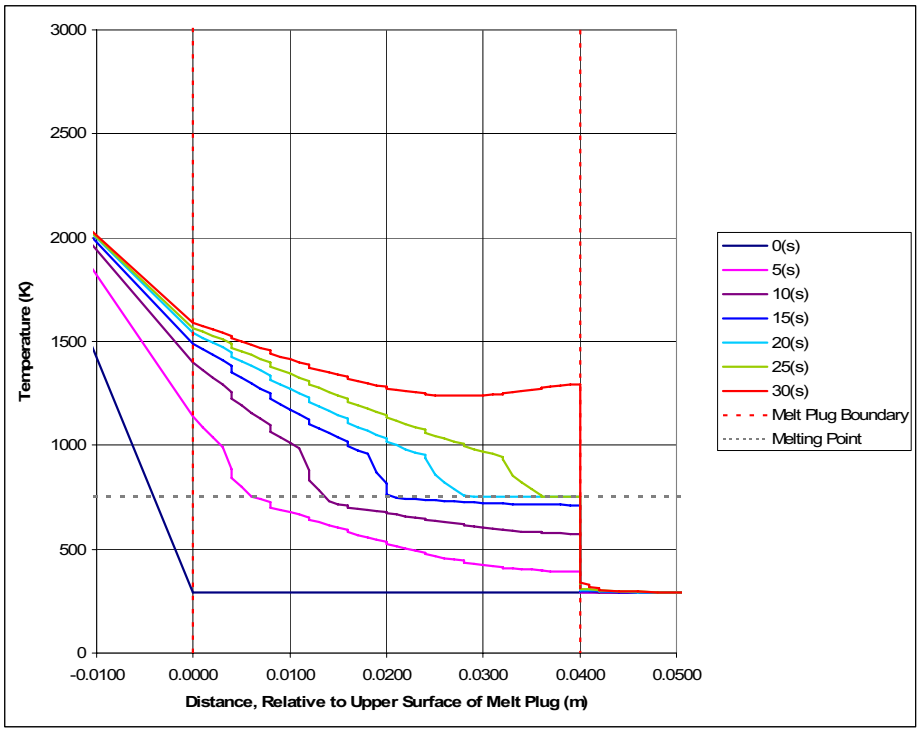

Figure 7-1 Aluminum Gate Temperature Profile with Oxidic Melt

7.3 *Results of Integral Analyses*

This section documents the integral plant response to the three bounding event scenarios described in Section 7.2.

7.3.1 *Large Break Loss of Coolant Accident (LBLOCA)*

The predicted U.S. EPR response during an LBLOCA event described in Section 7.2 is provided in Figures 7-5 to 7-27. The sequence of events and important results are provided in Table 7-2 and Table 7-3, respectively.

Table 7-2 Event Progression of a LBLOCA

[ ]

Table 7-3 Key Results from a LBLOCA

[ ]

Figure 7-5 Core Outlet Temperature (LBLOCA)

Figure 7-6 Two-Phase Water Level in Core (LBLOCA)

Figure 7-7 RCS Pressure (LBLOCA)

Figure 7-8 RCS Water Inventory (LBLOCA)

Figure 7-9 In-Vessel Hydrogen Production (LBLOCA)

Figure 7-10 Hydrogen Release Rate (LBLOCA)

Figure 7-11 Mass of Corium in Lower Head (LBLOCA)

Figure 7-12 Mass of Material in Core (LBLOCA)

Figure 7-13 Mass of Material in Lower Head and Core (LBLOCA)

Figure 7-14 Containment Pressure (LBLOCA)

Figure 7-15 Average H_2 and CO Mole Fraction in Containment (LBLOCA)

Figure 7-16 Average Mole Fraction of Air in Containment (LBLOCA)

Figure 7-17 Average Mole Fraction of Steam in Containment (LBLOCA)

Figure 7-18 Hydrogen Mass in Containment (LBLOCA)

Figure 7-19 Mass of Corium in Reactor Cavity (LBLOCA)

Figure 7-20 Mass of Corium in Spreading Compartment (LBLOCA)

Figure 7-21 Spreading Room Ablation (LBLOCA)

Figure 7-22 Reactor Cavity Ablation (LBLOCA)

Figure 7-23 Spreading Room Water Level (LBLOCA)

Figure 7-24 IRWST Water Level (LBLOCA)

Figure 7-25 Corium Temperature in Reactor Pit (LBLOCA)

Figure 7-26 Containment Spray Flow (LBLOCA)

Figure 7-27 SAHRS Suction Temperature (LBLOCA)

7.3.2 *Loss of Off-site Power*

The predicted U.S. EPR response during a SBO event described in Section 7.2 is provided in Figures 7-28 to 7-50. The sequence of events and important results are provided in Table 7-4 and Table 7-5 , respectively.

Table 7-4 Event Progression of a SBO

Table 7-5 Key Results from a SBO

Figure 7-28 Core Outlet Temperature (SBO)

Figure 7-29 RCS Pressure (SBO)

Figure 7-30 RCS Water Inventory (SBO)

Figure 7-31 Two-Phase Water Level in Core (SBO)

Figure 7-32 In-Vessel Hydrogen Production (SBO)

Figure 7-33 Hydrogen Release Rate (SBO)

Figure 7-34 Mass of Corium in Lower Head (SBO)

Figure 7-35 Mass of Material in Core (SBO)

Figure 7-36 Mass of Material in Lower Head and Core (SBO)

Figure 7-37 Containment Pressure (SBO)

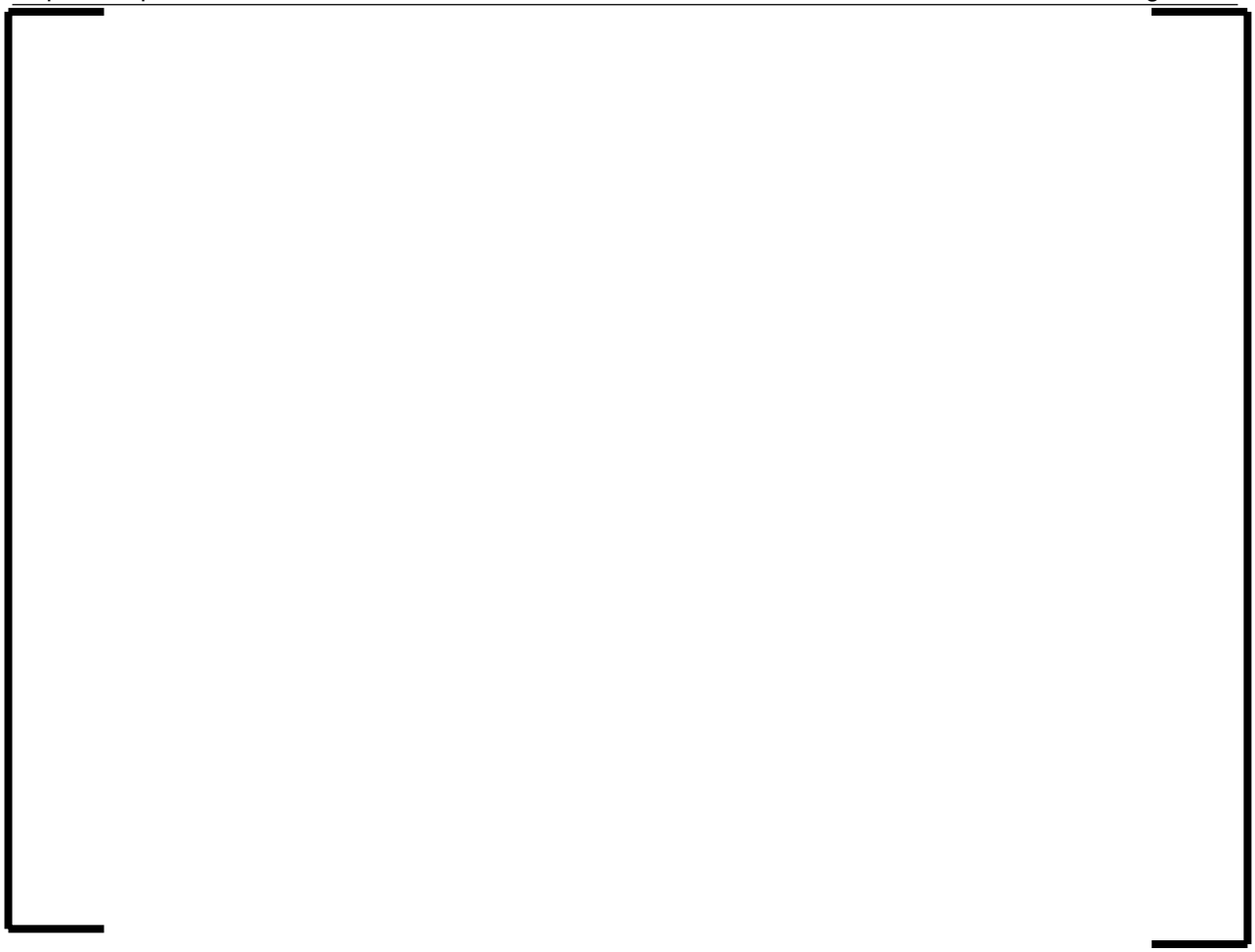

Figure 7-38 Average H_2 and CO Mole Fraction in Containment (SBO)

Figure 7-39 Average Mole Fraction of Air in Containment (SBO)

Figure 7-40 Average Mole Fraction of Steam in Containment (SBO)

Figure 7-41 Hydrogen Mass in Containment (SBO)

Figure 7-42 Mass of Corium in Reactor Pit (SBO)

Figure 7-43 Mass of Corium in Spreading Compartment (SBO)

Figure 7-44 Spreading Room Ablation (SBO)

Figure 7-45 Reactor Cavity Ablation (SBO)

Figure 7-46 Spreading Room Water Level (SBO)

Figure 7-47 IRWST Water Level (SBO)

Figure 7-48 Corium Temperature in Reactor Pit (SBO)

Figure 7-49 Containment Spray Flow (SBO)

Figure 7-50 SAHRS Suction Temperature (SBO)

7.3.3 *Small Break Loss of Coolant Accident (SBLOCA)*

The predicted U.S. EPR response during an SBLOCA event described in Section 7.2 is provided in Figures 7-51 to 7-73. The sequence of events and important results are provided in Table 7-6 and Table 7-7, respectively.

Table 7-6 Event Progression of a SBLOCA

[ ]

Table 7-7 Key Results from a SBLOCA

[ ]

Figure 7-51 Core Outlet Temperature (SBLOCA)

Figure 7-52 RCS Pressure (SBLOCA)

Figure 7-53 RCS Water Inventory (SBLOCA)

Figure 7-54 Two-Phase Water Level in Core (SBLOCA)

Figure 7-55 In-Vessel Hydrogen Production (SBLOCA)

Figure 7-56 Hydrogen Release Rate (SBLOCA)

Figure 7-57 Mass of Corium in Lower Head (SBLOCA)

Figure 7-58 Mass of Material in Core (SBLOCA)

Figure 7-59 Mass of Material in Lower Head and Core (SBLOCA)

Figure 7-60 Containment Pressure (SBLOCA)

Figure 7-61 Average H_2 and CO Mole Fraction in Containment (SBLOCA)

Figure 7-62 Average Mole Fraction of Air in Containment (SBLOCA)

Figure 7-63 Average Mole Fraction of Steam in Containment (SBLOCA)

Figure 7-64 Hydrogen Mass in Containment (SBLOCA)

Figure 7-65 Mass of Corium in Reactor Pit (SBLOCA)

Figure 7-66 Mass of Corium in Spreading Compartment (SBLOCA)

Figure 7-67 Spreading Room Ablation (SBLOCA)

Figure 7-68 Reactor Pit Ablation (SBLOCA)

Figure 7-69 Spreading Compartment Water Level (SBLOCA)

Figure 7-70 IRWST Water Level (SBLOCA)

Figure 7-71 Corium Temperature in Reactor Pit (SBLOCA)

Figure 7-72 Containment Spray Flow (SBLOCA)

Figure 7-73 SAHRS Suction Temperature (SBLOCA)

9.0 REFERENCES

1. U. S. NRC Standard Review Plan, NUREG-0800, most recent revision.

2. Fauske and Associates, Inc., 1994a. MAAP4—Modular Accident Analysis Program for LWR Power Plants, vol. 2, Part 1: Code Structure and Theory, prepared for Electric Power Research Institute, May 1994.

3. Sandia National Laboratories, NUREG/CR-6119, Rev. 2, MELCOR Computer Code Manuals, vol. 1: Primer and User's Guide, Version 1.8.5, Prepared by Sandia National Laboratories for the U.S. Nuclear Regulatory Commission, Office of Nuclear Regulatory Research, 2000.

4. U. S. Code of Federal Regulations, most recent revision.

5. US NRC, Policy Statement on Severe Reactor Accidents Regarding Future Designs and Existing Plants, Volume 50, page 32138, of the Federal Register dated August 8, 1985.

6. US NRC, Policy Statement on Safety Goals for the Operations of Nuclear Power Plants, Volume 51, page 28044, of the Federal Register, dated August 4, 1986.

7. US NRC, Policy Statement on Nuclear Power Plant Standardization, Volume 52, page 34844, of the Federal Register dated September 15, 1987.

8. US NRC, Policy Statement on The Use of Probabilistic Risk Assessment Methods in Nuclear Regulatory Activities, Volume 60, page 42622, of the Federal Register, dated August 16, 1995.

9. US NRC, SECY-90-016, "Evolutionary Light Water (LWR) Certification Issues and Their Relationship to Current Regulatory Requirements," issued January 12, 1990, and the corresponding staff requirements memorandum (SRM), issued June 26, 1990.

10. US NRC, SECY-93-087, "Policy, Technical, and Licensing Issues Pertaining to Evolutionary and Advanced Light-Water (ALWR) Designs," issued April 2, 1993, and the corresponding SRM, issued July 21, 1993.

11. Sauvage, E.C., et al., "OSSA – An Optimized Approach to Severe Accident Management: EPR Application," Proceedings of ICAPP '06, Reno, NV, June 2006.

12. Pilch, M. M., Yan, H., Theofanous, T. G., "The Probability of Containment Failure by Direct Containment Heating in Zion," NUREG/CR-6075, SAND93-1535, December 1994.

101. Huhtiniemi, I. and Magallon, D., Insight into Steam Explosions with Corium Melts in KROTOS, Nuclear Engineering and Design, 204, pp.391-400, 2001.

102. Kim, J. H., et al., “A Study on Intermediate Scale Steam Explosion Experiments with Zirconia and Corium Melts,” Transactions of the International Congress on Advanced Nuclear Power Plants (ICAPP), Hollywood, FL, June 9-13, 2002.

103. Song, J. H., Kim, J. H., Min, B. T., and Hong, S. W., “An Effect of Corium Composition Variations on Occurrence of a Spontaneous Steam Explosion in the TROI Experiments,” The 6th International Conference on Nuclear Thermal Hydraulics, Operations and Safety (NUTHOS-6), Nara, Japan, October 4-8, 2004.

104. EPRI TR-103413, “The MELTSPREAD-1 Computer Code for the Analysis of Transient Spreading and Cooling of High-Temperature Melts – Code Manual,” December 1993.

105. AREVA NP Inc. Technical Document, 38-9008026-000, “Description, Verification and Application of the Computer Code WALTER,” December 2005.

106. AREVA NP Inc. Technical Document, 38-9026695-000, “Development of MAAP4 Models for EPR-Specific Plant Design Features."

107. Baker, L., Faw, R. E., and Kulacki, F. A., “Post-accident Heat Removal – Part I: Heat Transfer Within an Internally Heated, Non-boiling Liquid Layer,” Nuclear Science and Engineering, 61, pp. 222-230, 1976.

108. Thompson, D. H. and Fink, J. K., "ACE MCCI Test L2: Test Data Report Volume I - Thermal Hydraulics," Argonne National Laboratory, November 1988.

109. Thompson, D. H. and Fink, J. K., "ACE MCCI Test L6: Test Data Report Volume I - Thermal Hydraulics," Argonne National Laboratory, August 1991.

110. Thompson, D. H. and Fink, J. K., "ACE MCCI Test L7: Test Data Report Volume I - Thermal Hydraulics," Argonne National Laboratory, November 1991.

111. Alsmeyer, H. and Firnhaber, M., "Specification of the International Standard Problem ISP-30: BETA V5.1 Experiment on Melt_Concrete Interaction," KfK and GRS, September 1990.

112. Alsmeyer, H., "Report on Recent BETA Experiments V5.1, V5.2 & V6.1," CSARP Meeting, Bethesda, MD, May 6-10, 1991.

113. Theofanous, T. G., Amarasooriya, W. H., Yan, H., and Ratnam, U., "The Probability of Liner Failure in a Mark I Containment," NUREG/CR-5423, 1990.